Optimizing Primary Response in Preventive Security-Constrained Optimal Power Flow

Yury Dvorkin, *Student Member, IEEE*, Pierre Henneaux, *Member, IEEE*, Daniel S. Kirschen, *Fellow, IEEE*, and Hrvoje Pandžić, *Member, IEEE*

***Abstract*—Preventive security-constrained optimal power flow (PSCOPF) dispatches controllable generators at minimum cost while ensuring that the system adheres to all operating constraints. All the transmission and generation limits are respected during both the pre- and post-contingency states without relying on post-contingency redispatch. Therefore, all credible generation contingencies should be modeled in PSCOPF and the system-wide automatic primary response should be allocated accordingly among synchronized generators by adjusting their droop coefficients. This paper proposes a new PSCOPF model that optimizes the droop coefficients of the synchronized generators. The cost savings attained with the proposed approach and its computational performance are evaluated. Different wind penetration levels and reserve policies are tested using annual simulations on the one- and three-area IEEE Reliability Test System.**

***Index Terms*—Optimal power flow, power system economics, power system security, primary frequency regulation.**

NOMENCLATURE

Indices and Sets

$n \in \mathbb{N}$	Index and the set of nodes.
$k \in \mathbb{K}$	Index and the set of branches (transmission lines and transformers).
$g \in \mathbb{G}$	Index and the set of generators.
$d \in \mathbb{D}$	Index and the set of loads.
$c \in \mathbb{C}$	Index and the set of operating states of the system, where $c = 0$ denotes the pre-contingency state without contingency, and $c = c_g$ denotes the post-contingency state with outage of generator g.

Variables

θ_{nc}	Voltage angle at node n in system state c.
P_{gc}	Active power supplied from generator g in system state c.
P_{nw}	Effective wind power generation at node n.
P_{kc}	Active power flow through transmission element k in system state c.
$z_{gc_{g'}}$	Binary variable equal to 1 if generator g produces its maximum output in state $c_{g'}$ and 0 otherwise.
$\Delta f_{c_{g'}}$	Power system frequency deviation in state $c_{g'}$ (primary regulation).
TC	Total cost.
ϵ_k	Positive slack variable for the rating of transmission element k.
x_{gi}	Binary variable equal to 1 if the frequency regulation constant of generator g is equal to d_i, and 0 otherwise.
$\alpha_{c_{g'}gi}$	Negative variable equal to the product of $\Delta f_{c_{g'}}$ by x_{gi}.

Parameters

$\theta^{\min}/\theta^{\max}$	Minimum/maximum voltage angle.
$P_g^{\min}/P_g^{\max}$	Minimum/maximum active power generation of generator g.
P_n^w	Wind generation available at node n.
$P_n^{f\_w}$	Wind generation forecast at node n.
$P_k^{\max}/\tilde{P}_k^{\max}$	Rating of transmission element k under normal/contingency conditions.
P_n^d	Active power load at node n.
$C_g(P)$	Cost of production of generator g when its power output is P.
B_k	Electrical susceptance of transmission element k.
D_g	Frequency regulation constant of generator g (primary regulation).
s_g	Frequency droop of generator g.
f^0	Nominal frequency of the power system.
d_i	Possible values for the frequency regulation constant.
I_{nk}	Incidence matrix whose elements are equal to 1 if branch k starts at node n, -1 if it ends at node n, and 0 otherwise.
1_{ng}	Binary indicator matrix whose elements are equal to 1 if generator g is connected to node n, and 0 otherwise.
1_{gc}	Binary indicator matrix whose elements are equal to 0 if the outage of generator g is a contingency in system state c, and 1 otherwise.

Manuscript received September 01, 2015; revised November 18, 2015; accepted February 06, 2016. Date of publication March 02, 2016; date of current version March 23, 2018. All the authors contributed equally to this work.

Y. Dvorkin and D. S. Kirschen are with the Department of Electrical Engineering, University of Washington, Seattle, WA 98195 USA (e-mail: iouridvorkin@gmail.com; kirschen@uw.edu).

P. Henneaux is with Tractebel Engineering (GDF-Suez), 1200 Brussels, Belgium, and also with the École polytechnique de Bruxelles, Université libre de Bruxelles, 1050 Brussels, Belgium (e-mail: pierre.henneaux@ulb.ac.be).

H. Pandžić is with the Faculty of Electrical Engineering and Computing, University of Zagreb, 10000 Zagreb, Croatia (e-mail: hrvoje.pandzic@fer.hr).

Digital Object Identifier 10.1109/JSYST.2016.2527726

I. INTRODUCTION

SECURITY-constrained optimal power flow (SCOPF) [1] optimizes the operating cost in the pre-contingency state and ensures that operating limits would be satisfied in the post-contingency steady state. The preventive SCOPF (PSCOPF) [2], [3], which assumes that the post-contingency steady-state conditions can be met without redispatching, dominates among

real-life SCOPF applications [4]. Indeed, following any single contingency, power flows and voltages need to remain within operating limits [5]. Even short-term transmission line overloads increase the likelihood of blackouts, because overcurrent and distance relays can trip protected elements in a few seconds [6]. Existing methods to PSCOPF are reviewed in [7].

While some corrective SCOPF (CSCOPF) models account for both the generation and transmission contingencies, it is not the case with the existing PSCOPF models. These typically consider only transmission contingencies [8]–[10] and do not explicitly model generator failures, although the latter ones have been shown to increase the pre-contingency operating cost [11]. Additionally, the discussions in [12], [13] point out that generators respond differently to line and generator outages and that the issue of generator contingencies should be accounted for in the PSCOPF. Inspired by discussions in [12] and [14], this paper argues that generator contingencies must be considered in the PSCOPF. It proposes an optimization model that ensures the allocation of primary response in a way that keeps power flows through transmission elements within the allowed limits immediately after any single generator contingency. This proposition is consistent with computationally effective solving strategies proposed in [2] and [3].

In the following, the *primary response* is defined as the automatic speed-governor-operated response [15] of synchronized generators intended to compensate the energy imbalance caused by the sudden failure of a generator [16]. Generator outages are normally considered to be part of the set of *credible contingencies*. The need for the system to continue operating satisfactorily through these contingencies determines its primary response requirement, which depends on the size and generation mix of the system as well as the economic considerations [16]–[18]. The most common requirement is that the primary reserve should be sufficient for the system to sustain the sudden outage of the largest synchronized generator; however, some system operators enforce more stringent requirements. For example, in ERCOT, the primary response requirement is 2300 MW, which prevents load shedding upon the simultaneous loss of the two largest generation resources [19]. In ERCOT, NYISO, WECC, and PJM, all synchronized and eligible generators must contribute to the provision of primary response by having their turbine governors in service and unblocked [20].

The contribution of a generator to primary response is determined by its droop coefficient, which is usually set at the same value for all generators [15]. Restrepo *et al.* [21] account for the primary response at the day-ahead unit commitment stage using an MIP model of the turbine speed governor and assume that all generators have the same droop coefficient. These authors co-optimize primary response and tertiary reserve but ignore transmission constraints, which may result in violations of network constraints when primary response is deployed in real time. Doherty *et al.* [22] amend the model of the turbine speed governor in [21] by formulating a day-ahead UC model with rate of change of frequency (Rocof) constraints.

The standard droop coefficients differ between interconnections but typically range from 2% to 6% [21]. In some power systems, droop coefficients are required to be adjustable in a larger range: from 2% to 8% in Saudi Arabia [24] and even from 2% to 12% in Norway [25]. Droop parameters are usually set at the commissioning of the generators and not modified after. However, modern control devices make it possible to change the droop coefficient of a generator in real time [26]–[28]. The compulsory provision of primary reserve with constant droop coefficients is not necessarily cost effective [29] and does not provide an incentive to generating units to provide primary response [30]–[32]. This raises some reliability concerns. For instance, some turbine control systems may override the turbine speed governor control loop, which may seriously affect the system-wide primary response [33], [34]. Ingleson *et al.* [34] analyzed the large generation outages that occurred from 1994 to 2004 and observed that the primary response in the US Eastern Interconnection reduced from 37.5 MW/mHz in 1994 to 30.7 MW/mHz in 2004. Du *et al.* [35] analyzed PMU measurements obtained during large generation contingencies in the WECC system and concluded that the primary response of generators has reduced due to more renewable generation. Since renewable generation replaces base-load controllable generators which provide most of primary response, high levels of wind generation may affect a power system's operational reliability [22], [23]. This problem can be somewhat alleviated if each balancing authority is required to provide its own primary response [35]. However, a case study on a relatively small isolated system [22] showed that, under some conditions, available wind generation must be curtailed to ensure the provision of an adequate amount of primary response. Observations in [22], [33]–[35] suggest that the compulsory provision of primary response is likely to limit the ability of power systems to accommodate wind power injections. In line with [22], [33]–[35], Illian [36] concludes that methods that will indicate the contribution of each generator to primary response should be investigated. This paper argues that the contribution of each generator to the overall system primary response must be determined by co-optimizing the droop coefficients with the rest of the PSCOPF decisions. This approach takes into account the characteristics of the synchronized generators and the network constraints in the allocation of the responsibilities for primary response.

This paper makes the following contributions:

1) It formulates a PSCOPF model that explicitly models generator contingencies in a vertically integrated environment, thus leaving out market implications of the primary response provision.
2) The proposed PSCOPF model optimally allocates primary response among synchronized generators to respect network constraints by adjusting the droop coefficients of individual generators. These coefficients can be optimized on an hourly or daily basis.
3) A Benders-type decomposition is implemented to reduce computing times. The near-optimality of the results obtained with this approximation is demonstrated by comparing them with those obtained using the full formulation of the PSCOPF model on the IEEE Reliability Test System (RTS).
4) The proposed method is then used to assess reserve policies for primary response for large wind penetrations (in this paper term, *wind penetration* refers to the ratio of the

available wind energy and the total load). In this analysis, we conclude that the proposed PSCOPF model can be paired with refined contingency reserve policies (CRP) to reduce the overall operating costs.

The remainder of this paper is organized as follows. Section II uses a two-bus example to explain the motivation for the proposed PSCOPF and the optimization of the droop coefficients. Section III describes the modeling of generator contingencies in the PSCOPF formulation. Section IV explains the optimization of droop coefficients within the PSCOPF. Section V assesses the cost savings and the computational performance achievable with the proposed approach.

II. Motivation and Concept

When a generator outage occurs, the system frequency drops quickly because of the imbalance between load and generation. The automatic primary response is activated automatically [16], [37] to keep the frequency above the level at which underfrequency load shedding is triggered [37]. If the outage of generator g causes a frequency drop Δf_{c_g}, each remaining synchronized generator g automatically increases its output by ΔP_{gc_g}:

$$\Delta P_{gc_g} = \min\left(-D_g \Delta f_{c_g}, P_g^{\max} - P_{g0}\right) \tag{1}$$

where D_g, $P_g^{\max}$, and P_{g0} are, respectively, the frequency regulation constant, the maximum power limit, and the pre-contingency output of that generator g. The automatic primary response of each generator g is thus proportional[1] to D_g and only constrained by the maximum power limit of that generator. Alternatively, the contribution of generator g to primary response can be defined using its droop s_g, i.e., the relative frequency deviation that causes primary response $P_{gc_g} = P_g^{\max}$:

$$s_g = -\frac{\Delta f_{c_g}/f^0}{\Delta P_{gc_g}/P_g^{\max}} \tag{2}$$

where f^0 is the nominal frequency [39]. This droop coefficient is generally expressed in % and is related to the frequency regulation constant as follows:

$$s_g = \frac{P_g^{\max}}{f^0 D_g}. \tag{3}$$

Since the primary response of generator g is automatic and only constrained by $P_g^{\max}$, its deployment may result in transmission overloads [40]. The primary response of each generator g should therefore be co-optimized with the generation dispatch in the PSCOPF so that the transmission constraints are satisfied in the post-contingency steady state without the need for redispatch.

The two-bus example in Fig. 1 illustrates this issue. Generators G1 and G2 have the same incremental production cost of \$20/MWh. Generator G3 has an incremental production cost of \$10/MWh, and its ability to supply the load at bus 1

[1]Although the primary response characteristic is generally nonlinear, linear approximations are used in practice [38].

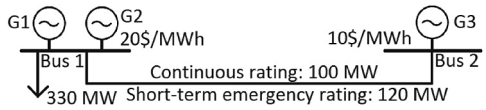

Fig. 1. Two-bus system diagram.

in the pre-contingency state is limited by the flow limit on the transmission line connecting buses 1 and 2. The continuous and short-term emergency ratings of transmission line 1–2 are 100 and 120 MW, respectively. For simplicity, all generators are assumed to have an unlimited capacity and the same droop coefficients. Solving the OPF problem with no security constraints suggests that generators G1, G2, and G3 should produce 115, 115, and 100 MW, respectively, resulting in a total cost TC^{OPF} =\$5600/h. However, if generator G1 trips, generators G2 and G3 will each have to provide 57.5 MW of primary response, which would overload line 1–2 (100 + 57.5 = 157.5 MW >120 MW). On the other hand, if generator contingencies are included in the PSCOPF, generators G1, G2, and G3 would produce 140, 140, and 50 MW, respectively, and the total operating cost would be $\text{TC}^{\text{PSCOPF}}$ =\$6100/h. In this case, if generator G1 trips, G2 and G3 will each provide 70 MW of primary response and the post-contingency power flow in transmission line 1–2 will remain within its short-term emergency rating. Accounting for generation contingencies in the PSCOPF avoids violating transmission constraints. The increase in the operating cost of the PSCOPF solution is attributed to the higher security cost (SC), i.e., the difference between the cost of PSCOPF and the cost of OPF ($\text{SC}^{\text{PSCOPF}} = \text{TC}^{\text{PSCOPF}} - \text{TC}^{\text{OPF}} = 6100 - 5600 = \$500/\text{h}$).

This security cost can be reduced by optimizing the droop coefficients of generators. Including the droop coefficients in the set of decision variables provides additional flexibility in the PSCOPF and hence a way to reduce the security cost. For example, if the droop settings must remain within the range 2–12% [25], the PSCOPF would dispatch G1, G2, and G3 at 120, 120, and 90 MW and set their droop coefficients at 2%, 2%, and 6%, respectively. The total cost $\text{TC}^{\text{PSCOPF,opt}}$ would then be \$5700/h and the security cost $\text{SC}^{\text{PSCOPF,opt}} = \text{TC}^{\text{PSCOPF,opt}} - \text{TC}^{\text{OPF}}$ would be only \$100/h. Under these conditions, following the outage of G1, G2, and G3 would increase their outputs by 90 and 30 MW, respectively, and the post-contingency flow in line 1–2 would be limited to 120 MW, i.e., its short-term emergency rating. Figs. 2 and 3 show the security cost (SC) and the relative security cost (RSC) achieved by the PSCOPF with fixed and optimized droop coefficients as a function of the load at bus 1. The relative security cost is defined as $\text{RSC} = \text{SC}^{\text{PSCOPF}}/\text{TC}^{\text{OPF}} \times 100\%$. Since light loads do not cause congestion, security can be achieved at no cost and optimizing droop is an unnecessary control option (region I in Figs. 2 and 3). As the load increases, optimizing the droop coefficients makes it possible to meet the security constraints at a lower cost (region II). As the load increases even further (region III), the benefit derived from the optimization of the droop coefficients decreases because of the limits on the acceptable range of droop coefficients.

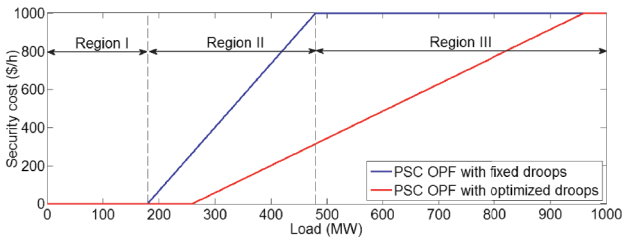

Fig. 2. Security cost (SC, $/h) incurred by the PSCOPF with variable and fixed droop coefficients.

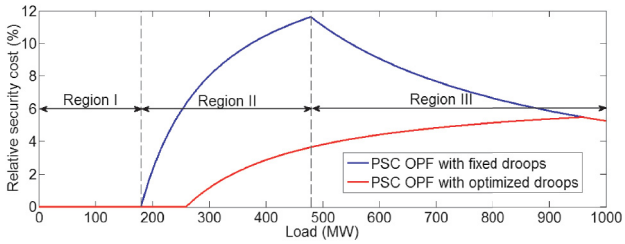

Fig. 3. Relative security cost (RSC, %) incurred by the PSCOPF with variable and fixed droop coefficients.

III. PSCOPF With Generator Contingencies

A. PSCOPF Formulation

The PSCOPF aims to minimize the operating cost in the pre-contingency steady state ($c = 0$):

$$\min_{P_{g0}} \sum_{g} C_g(P_{g0}) \tag{4}$$

where $C_g(\cdot)$ is the cost function of generator g and P_{g0} is its pre-contingency power output. This optimization is subject to the following constraints on the pre- and post-contingency states:

$$\sum_{g} 1_{ng} P_{gc} + P_n^{\mathrm{w}} + \sum_{k} I_{nk} P_{kc} = P_n^{\mathrm{d}} \quad \forall n, c \tag{5}$$

$$1_{gc} P_g^{\min} \le P_{gc} \le 1_{gc} P_g^{\max} \quad \forall g, c \tag{6}$$

$$0 \le P_n^{\mathrm{w}} \le P_n^{\mathrm{f\_w}} \quad \forall n \tag{7}$$

$$P_{kc} = B_k \sum_{n} I_{nk} \theta_{nc} \quad \forall k, c \tag{8}$$

$$-P_{kc}^{\max} \le P_{kc} \le P_{kc}^{\max} \quad \forall k, c \tag{9}$$

$$\theta^{\min} \le \theta_{nc} \le \theta^{\max} \quad \forall n > 1, c \tag{10}$$

$$\theta_{1c} = 0 \quad \forall c \tag{11}$$

$$P_{gc_g} \ge z_{gc_g} P_g^{\max} \quad \forall g, c_g \tag{12}$$

$$P_{gc_g} \le 1_{gc_g} (P_{g0} - D_g \Delta f_{c_g}) \quad \forall g, c_g \tag{13}$$

$$P_{gc_g} \ge 1_{gc_g} (P_{g0} - D_g \Delta f_{c_g}) - M z_{gc_g} \quad \forall g, c_g. \tag{14}$$

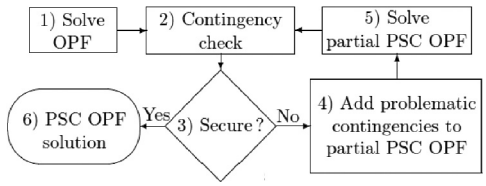

Fig. 4. Solution algorithm for the PSCOPF.

Equation (5) enforces the power balance at each node n of the system. Constraint (6) enforces the minimum and maximum limits on the generators' outputs. Constraint (7) limits the output of the wind farms to the forecast value $P_n^{f\text{-}w}$. Equation (8) calculates the dc power flows, and (9) enforces the flow limits on each transmission line k. Constraints (10), (11) limit the voltage angles at buses $n > 1$ and set the voltage angle at the reference bus $n = 1$ to 0. The choice of $\theta^{\min}$ and $\theta^{\max}$ can be tailored to a given network to ensure that the assumption on the small angle approximation used in the dc power flow model holds. This tuning is of great importance in large-scale sparse networks. Constraints (5)–(11) are enforced for $\forall c$, so that these limits are enforced for the pre- ($c = 0$) and post-contingency ($c > 0$) states. Constraints (12)–(14) model the primary response after contingency c, as explained in [21]. If binary variable $z_{gc_g} = 0$, (12) is always satisfied and (13) and (14) are reduced to $P_{gc_g} = 1_{gc_g}(P_{g0} - D_g \Delta f_{c_g})$. On the other hand, if binary variable $z_{gc_g} = 1$, (14) is not binding and (12), combined with (6), limits the primary response to $P_{gc_g} = P_g^{\max}$. The proposed PSCOPF assumes that dynamic stability controls are sufficient to transition the system between the pre- and post-contingency steady states [38].

The proposed PSCOPF model treats wind power generation in a deterministic fashion. However, it can be modified to model wind power generation uncertainty using stochastic, interval, and robust optimization. As demonstrated in [41], [42], these techniques may incur unnecessary computational complexity. The complexity of the optimization problem (4)–(14) increases with the number of contingencies. However, only a few contingencies are typically binding [10]. Therefore, this optimization problem can be solved efficiently using the algorithm proposed in [1] and shown in Fig. 4. First, the OPF is solved, followed by the contingency check, which determines whether the OPF solution is feasible for each contingency c. If the contingency check detects that the OPF solution is not acceptable for some contingencies, these contingencies are added to the partial PSCOPF. This partial PSCOPF is solved, and the contingency check is performed again. Steps 2–5 are repeated until the algorithm in Fig. 4 returns a fully secure solution, i.e., a solution satisfying constraints (5)–(14). Since the partial PSCOPF considers only the contingencies that are infeasible under the OPF solution, it involves less contingencies than a full PSCOPF, and therefore, it can be solved faster [1].

B. Decomposed PSCOPF Formulation

The authors of [9], [43] use Benders' decomposition to solve the SCOPF problem. Their formulations decompose the SCOPF into a master problem for the pre-contingency state and a set of subproblems for each transmission line contingency

considered. The master problem solves an OPF and its solution is passed on to the subproblems which check the feasibility of the OPF solution for each contingency. Each infeasible subproblem uses slack variables to generate a Benders' cut that is returned to the master problem as an additional constraint to make the corresponding subproblem feasible. The procedure is repeated until all subproblems are feasible, and the values of the slack variables are below a given tolerance. Both the master problem and all the subproblems are convex in the formulation of [9]. This guarantees that the Benders' decomposition produces the optimal solution of the original problem [44], [45]. Modeling generation contingencies makes the problem more computationally challenging because of a larger number of contingencies considered than in the PSCOPF with transmission contingencies only and because of the generator output limits. These limits require the introduction of binary variable z_{gc_g} in (12) and (14). The presence of these binary variables makes the problem nonconvex and the optimality of the solution obtained using Benders' decomposition cannot be guaranteed. However, as in [46], a Benders-type approach can be used to decompose the optimization problem (4)–(14) into a convex master problem and nonconvex subproblems. Although this leads to a near-optimal solution, the computation time is improved to scale the PSCOPF for large networks. In this work, we validate the usefulness of this decomposition via numerical simulations, showing the cost savings achieved with the proposed PSCOPF. As in [9] and [43], the master problem solves the OPF for the pre-contingency steady state ($c = 0$) and is thus convex:

$$\min_{P_{g0}} \sum_{g} C_g(P_{g0}) \tag{15}$$

subject to:

$$\text{constraints } (5)-(11), c = 0 \quad \forall n, k, g. \tag{16}$$

The nonconvex subproblems model the primary response for every generation contingency (c_g):

$$\min_{\epsilon_k} \sum_{k} \epsilon_k \tag{17}$$

subject to:

$$\text{Constraints } (5), (6), (8), (10), (12)-(14) \quad \forall n, k, g, c_g \tag{18}$$

$$P_{g0} = P^*_{g0} \quad \forall g \tag{19}$$

$$P^{\mathrm{w}}_{n} = P^{\mathrm{w}*}_{nw} \quad \forall n \tag{20}$$

$$-\left(P^{\max}_{kc_g} + \epsilon_k\right) \leq P_{kc_g} \leq \left(P^{\max}_{kc_g} + \epsilon_k\right) \quad \forall k, c_g \tag{21}$$

$$\epsilon_k \geq 0. \tag{22}$$

The constraints listed under (18) enforce limits on the generation and transmission assets for each contingency c_g. Equations (19) and (20) set the pre-contingency power output of generator g and wind farm w at node n to the solution of the master problem P^*_{g0} and P^*_{nw}. Constraint (21) is obtained from (9) by introducing a slack variable ϵ_k enforced to be positive by (22). Therefore, if contingency c_g violates the flow limit $P^{\max}_{kc}$, slack variable ϵ_k will be greater than zero and zero otherwise. Each subproblem is feasible if $\sum_k \epsilon_k \leq \epsilon$, where ϵ is a predefined tolerance. If $\sum_k \epsilon_k > \epsilon$, a Benders' cut of the following form is added to the master problem:

$$\sum_{k} \epsilon^*_k + \sum_{g} \lambda^p_g \left(P_{g0} - P^*_{g0}\right) + \sum_{n} \lambda^w_n \left(P^w_n - P^{w*}_n\right) \leq 0 \tag{23}$$

where ϵ^*_k is the optimized value of the slack variable, λ^p_g is the Lagrange multiplier of (19), and λ^w_n is the Lagrange multiplier of (20). λ^p_g and λ^w_n are provided by the solver at every iteration when the subproblem is solved. After adding the Benders' cut to the master problem, the procedure is repeated until a solution that is feasible within the given tolerance for all the subproblems is found.

IV. Droop Setting Optimization

A. Optimizing Primary Response in the PSCOPF

In the PSCOPF formulation presented in Section III-A, the primary response of each generator is exogenously set to a specific value. As illustrated in the two-bus example of Section II, optimizing D_g may reduce the operating cost while avoiding violation of the transmission constraints. However, if D_g is modeled as a continuous decision variable, the optimization problem (4)–(14) becomes nonlinear because constraints (13) and (14) involve the product of continuous variables D_g and Δf_{c_g}. To avoid this nonlinearity, the continuous variable D_g can be discretized as follows:

$$D_g = \sum_{i} x_{gi} d_i \quad \forall g \tag{24}$$

$$\sum_{i} x_{gi} = 1 \quad \forall g \tag{25}$$

where d_i is a parameter that discretizes the domain of D_g and x_{gi} is a binary decision variable. If $x_{gi} = 1$, D_g is uniquely set to d_i in (24), because (25) makes sure that only one element x_{gi} is equal to one for each generator g. After running a large number of simulations, we determined that the 1% droop step provides sufficient accuracy of the model without significant increase in computing time. However, in general, a finer resolution of this discretization may lead to more cost-effective decisions at the expense of increasing computing times.

Constraints (13) and (14) can now be recast as follows:

$$P_{gc_g} \leq 1_{gc_g} \left(P_{g0} - \sum_{i} x_{gi} d_i \Delta f_{c_g}\right) \quad \forall g, c'_g \tag{26}$$

$$P_{gc_g} \geq 1_{gc_g} \left(P_{g0} - \sum_{i} x_{gi} d_i \Delta f_{c_g}\right) - M z_{gc_g} \quad \forall g, c_g. \tag{27}$$

Constraints (26) and (27) involve the product of binary variable x_{gi} and continuous variable Δf_{c_g}. However, this type

of nonlinearity can be linearized by introducing a continuous variable $\alpha_{c_g gi}$:

$$\alpha_{c_g gi} \geq \Delta f_{c_g} \quad \forall c_g, g, i \tag{28}$$
$$\alpha_{c_g gi} \leq \Delta f_{c_g} + M(1 - x_{gi}) \quad \forall c_g, g, i \tag{29}$$
$$\alpha_{c_g gi} \geq -M x_{gi} \quad \forall c_g, g, i \tag{30}$$
$$\alpha_{c_g gi} \leq 0 \quad \forall c_g, g, i \tag{31}$$

which leads to the following linear reformulation of (26) and (27):

$$P_{gc_g} \leq 1_{gc_g} \left(P_{g0} - \sum_i \alpha_{c_g gi} d_i \right) \quad \forall g, c_g \tag{32}$$

$$P_{gc_g} \geq 1_{gc_g} \left(P_{g0} - \sum_i \alpha_{c_g gi} d_i \right) - M z_{gc_g} \quad \forall g, c_g. \tag{33}$$

The PSCOPF including droop settings is then formulated as follows:

$$\min_{P_{g0}} \sum_g C_g(P_{g0}) \tag{34}$$

subject to:

$$\text{constraints } (5)-(12), (25), (28)-(33) \quad \forall n, k, g, c. \tag{35}$$

B. Decomposed PSCOPF With Optimal Droop Settings

Even when only binding contingencies are included, the MIP model described in the previous section contains a large number of binary variables, which makes it computationally intractable. The approximate decomposition technique described in Section III-B can be adapted as follows. The master problem remains the same but with the addition of constraint (25). If we only replace (13), (14) by (28)–(33) in the subproblems with the additional constraint:

$$x_{gi} = x^*_{gi} \quad \forall g, i \tag{36}$$

where x^*_{gi} is the optimal value of x_{gi} found by the master problem, we cannot include variables x_{gi} in the infeasibility cut. This difficulty arises from the discretization of the droop settings: no Lagrange multiplier is associated with a constraint on binary variables. To estimate the impact of droop changes on the feasibility of subproblems, we introduce a real variable $\beta_{c_g gi}$ similar to $\alpha_{c_g gi}$ in (32) and (33):

$$P_{gc_g} \leq 1_{gc_g} \left(P_{g0} - \sum_i (\alpha_{c_g gi} + \beta_{c_g gi}) d_i \right) \quad \forall g, c_g \tag{37}$$

$$P_{gc_g} \geq 1_{gc_g} \left(P_{g0} - \sum_i (\alpha_{c_g gi} + \beta_{c_g gi}) d_i \right) - M z_{gc_g} \quad \forall g, c_g \tag{38}$$

under the condition that these variables are equal to 0:

$$\beta_{c_g gi} = 0 \quad \forall g, c_g, i. \tag{39}$$

A Lagrange multiplier is associated with this last constraint. It is equivalent to replacing $\beta_{c_g gi}$ by δ or increasing $\alpha_{c_g gi}$ by δ. As $\alpha_{c_g gi}$ represents the product of x_{gi} with Δf_{c_g}, it would be equivalent to change x_{gi} by $\delta / \Delta f_{c_g}$ if x_{gi} was real. Because the frequency deviation after a generator contingency (primary regulation) depends on the droop settings, this is not completely true: if x_{gi} changes, Δf_{c_g} changes. However, if the change in droop settings is small, the post-contingency frequency after a specific contingency Δf_{c_g} will not change significantly. We can thus construct the following infeasibility cut:

$$\sum_k \epsilon^*_k + \sum_g \lambda^p_g (P_{g0} - P^*_{g0}) + \sum_n \lambda^w_n (P^w_n - P^{w*}_n) + \sum_g \sum_i \lambda^x_{gi} (x_{gi} - x^*_{gi}) \leq 0 \tag{40}$$

where λ^x_{gi} is the Lagrange multiplier associated with constraint (39) divided by Δf_{c_g}.

This method is an approximation for two reasons: the Benders decomposition is inexact when subproblems are not convex and the hypothesis that Δf_{c_g} is insensitive to changes in droop settings is not strictly true. However, it makes possible the rapid co-optimization of the dispatch and droop settings under preventive security constraints.

V. Case Study

This section presents simulation results obtained on the one- and three-area IEEE RTS with the generation and transmission data from [47]. All PSCOPF computations were performed using the CPLEX 12.1 solver [48] in GAMS 24.0.2 environment [49] on a supercomputer system with 2.5-GHz Intel Xeon CPU L5420 processors and 16 GB RAM. The duality gap for each MILP problem was set to 1.5×10^{-3}.

A. One-Area RTS

The one-area IEEE RTS is used to compare the solution quality and the computational performance for the following three cases:

1) *Case I* uses the exact formulation presented in Section IV-A to co-optimize the generation dispatch and the variable droop coefficients.
2) *Case II* uses the approximate formulation presented in Section IV-B to co-optimize the generation dispatch decisions and the droop coefficients.
3) *Case III* uses the formulation presented in Section III-A to optimize the generation dispatch given the droop coefficients obtained from Case II. Thus, Case III aims to improve the optimality of the generation dispatch compared to Case II.

Case I solves the full MILP model and does not use the Benders-type decomposition, thus ensuring the global optimality. Since Cases II and III apply the Benders-type decomposition to a nonconvex subproblem, the global optimality is not guaranteed. However, the quality of the solutions of these cases can be assessed by comparing them to Case I. Cases I–III are tested with the same set of all $(N-1)$ contingencies.

For the following illustrative simulations, we assume that all generators are committed and participate in primary frequency

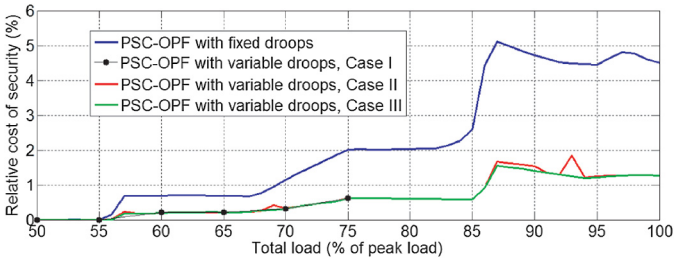

Fig. 5. RSC for the one-area RTS.

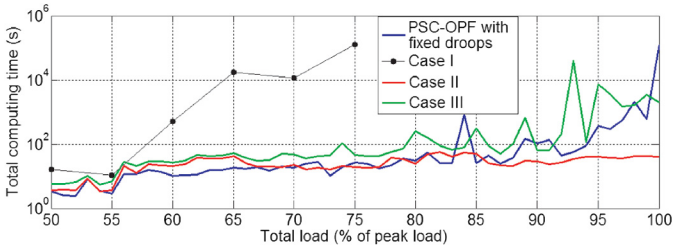

Fig. 6. Computation time for droop coefficient optimization.

TABLE I
PROPORTION OF HOURLY TIME INTERVALS WITH THE FEASIBLE PSCOPF

Contingency reserve policy	Wind penetration (%)	Fixed droop (%)	Hourly variable droop (%)	Daily variable droop (%)
CRP 1	10	92.77	92.82	92.82
	20	70.18	70.25	70.22
	30	60.33	60.42	60.42
CRP 2	10	100	100	100
	20	99.94	99.95	99.95
	30	99.52	99.59	99.55

control. We also reduce the power flow limits on the 400-kV transmission lines from 500 to 275 MW to create congested conditions.

Fig. 5 compares the relative security cost (RSC) of the different PSCOPF approaches to the nonsecure OPF solution for different load levels. The traditional PSCOPF with fixed droop coefficients consistently results in the largest RSC for load levels over 55% of the peak load, thus demonstrating the relative inefficiency of this approach. On the other hand, Cases I–III show that the PSCOPF outperforms the traditional approach and achieves a relatively constant RSC over all load levels. The RSC in Case II deviates in some places from the RSC of Cases I and III. This is attributable to the suboptimality of the Benders-type decomposition. However, Fig. 6 shows that Case II outperforms Cases I and III in terms of the computing times for all load levels. Case I cannot be solved within the 10^6 s limit on the execution time for load levels larger than 75% of the peak load, which justifies the implementation of the Benders-type decomposition for applications in system operation. On the other hand, the computing times of Cases II and III are comparable to those obtained for the PSCOPF with fixed droop coefficients, which uses the decomposed model described in Section III-B.

B. Three-Area IEEE RTS With Wind Generation

To assess the impact of variable droop coefficients on power system with high wind penetration, we perform simulations on the three-area IEEE RTS [47] for 10%, 20%, and 30% wind penetration levels. The simulations are performed day-by-day for an entire year. First, we solve the deterministic unit commitment (UC) as modeled in [50], additionally enforcing "$3 + 5$" reserve policy [51] for load and wind generation uncertainty and $(N-1)$ reserve policy for contingencies. We refer interested readers to the description of the 3BIN_MINUPDOWN UC model in [50] for the specific objective function and constraints used in this case study and to [52] for the day-to-day modeling of wind data. Motivated by [35], which argues that this traditional CRP should be revised, we compare two allocation strategies for the contingency reserve.

1) *Contingency Reserve Policy 1* (CRP1) mirrors the traditional practice and assumes that the three areas share the common $(N-1)$ contingency reserve requirement based on the largest generator committed in all three areas.
2) *Contingency Reserve Policy 2* (CRP2) uses the policy suggested in [35]. It assumes that each area provides at least a third of the $(N-1)$ contingency reserve requirements based on the largest committed generator in all three areas.

After solving the daily UC model with a specific reserve policy, we enforce its commitment decisions both in the nonsecure OPF and in the PSCOPF model implemented as explained in Case III of Section V-A. After evaluating the solution against the real-time realization of uncertainty, we compute the operating cost and the security cost attained for each approach. We then analyze the impact of optimal droop settings on the operating cost by comparing the results with fixed and optimized droop settings. Since some generators might not be able to change their droop coefficients on an hourly basis, we also consider the case where the droop setting of each generator is adjusted once a day.

After solving the UC model with a specific reserve policy, we enforce its commitment decisions both in the nonsecure OPF and in the PSCOPF model implemented as explained in Case III of Section V-A. After evaluating the solution against the real-time realization of uncertainty, we compute the operating cost and the security cost attained for each approach. We then analyze the impact of optimal droop settings on the operating cost by comparing the results with fixed and optimized droop settings. Since some generators might not be able to change their droop coefficients on an hourly basis, we also consider the case where the droop setting of each generator is adjusted once a day.

The binary decisions of the day-ahead UC do not necessarily ensure the feasibility of the PSCOPF. Table I shows the percentage of the hourly intervals during the course of the calendar year when the PSCOPF is feasible. These results show that the number of feasible states decreases as the wind penetration increases, for both CRP. This confirms the observations made in [35] and indicates that wind integration makes it more challenging to ensure $(N-1)$-secure operation. Under the 10% wind penetration level, the infeasibility of the PSCOPF model occurs

TABLE II
ANNUAL OPERATING COST (M$)

Contingency reserve policy	Wind penetration (%)	Fixed droop	Hourly variable droop	Daily variable droop
CRP 1	10	673.542	673.332	673.424
	20	562.103	561.616	561.776
	30	476.216	475.424	475.624
CRP 2	10	700.273	700.160	700.201
	20	591.521	590.116	590.314
	30	502.900	499.766	499.947

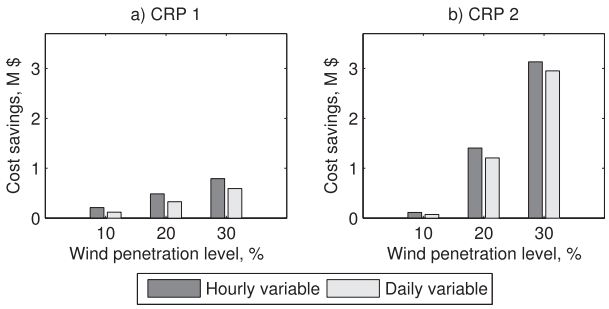

Fig. 7. Cost savings attained under different CPS and wind penetration levels.

TABLE III
ANNUAL SECURITY COST (M$)

Contingency reserve policy	Wind penetration (%)	Fixed droop	Hourly variable droop	Daily variable droop
CRP 1	10	0.579	0.368	0.460
	20	1.240	0.753	0.912
	30	1.698	0.907	1.106
CRP 2	10	0.123	0.009	0.050
	20	1.550	0.144	0.342
	30	4.059	0.925	1.107

TABLE IV
AVERAGE COMPUTING TIMES (S)

Contingency reserve policy	Wind penetration (%)	Fixed droop	Hourly variable droop	Daily variable droop
CRP 1	10	9	25	28
	20	74	34	34
	30	10	11	21
CRP 2	10	10	21	25
	20	14	33	35
	30	46	222	118

due to contingencies of U400 units that provide the largest power infeed to the network. If wind penetration is increased to 20% and 30%, the infeasibility of the PSCOPF model is mainly caused by a combination of contingencies on generator types U197 and U400. Optimizing the droop coefficients increases the number of feasible states for both CRP as compared to operation with fixed droop coefficients. The hourly variable droop optimization barely outperforms the daily droop optimization for some wind penetration levels. For hours with no feasible PSCOPF solution, in the following calculations, we adopt the nonsecure OPF solution.

Table II presents the annual operating costs for different wind penetration levels and CRP. The droop coefficient optimization reduces the annual operating cost for all wind penetration levels and for both CRP. Furthermore, we observe that the benefits of the droop optimization vary for different operating intervals. Thus, it reduces the operating cost up to 20.8% for CRP2 and a 30% wind penetration. The cost savings achieved through droop coefficient optimization are compared in Fig. 7 for hourly and daily droop adjustments. The proposed PSCOPF method results in larger cost savings for larger wind penetration levels and thus facilitates wind integration under both CRP. However, the cost savings achieved with droop coefficient optimization using CRP2 policy are an order of magnitude larger for high wind penetration levels than for the CRP1 policy. This observation suggests that if the traditional CRP1 policy is replaced by the CRP2 policy to improve the automatic primary response as demonstrated in [35], the proposed PSCOPF would result in larger cost savings. These cost savings are observed for both daily and hourly droop coefficient optimizations. Since hourly based optimization provides more flexibility for generation dispatch decisions, the average annual savings are up to 11.7% higher for daily droop setting optimization.

Table III summarizes the annual security cost for these various cases. Together with the results given in Table II, this suggests that the operational cost savings stemming from droop coefficient optimization result from a reduction in the security cost. Despite a lower operating cost, the traditional CRP1 leads to a larger security cost than the CRP2 for 10% and 20% wind penetration levels. However, at the 30% penetration level, the CRP2 incurs a larger security cost, if the proposed droop optimization is not used, due to the replacement of conventional generators providing primary response by wind power generators. On the other hand, if the droop optimization is used, the security cost gap between the CRP1 and CRP2 at the 30% wind penetration level nullifies as shown in Table III. Therefore, we conclude that the proposed PSCOPF with droop coefficient optimization and the CRP2 can be thought as mutually complementary tools for the cost-efficient provision of primary reserve in power system with high wind penetration levels.

The PSCOPF model with droop coefficient optimization is a mixed-integer linear program (MILP) and is generally NP-hard. Table IV presents the average computing times for each hourly interval during the calendar year considered. We the droop coefficient optimization in the PSCOPF is generally more computationally demanding than the PSCOPF with fixed droop coefficients. This increase in computing time is the result of introducing binary variable x_{gi} in (24) and (25) to discretize the domain of possible values of droop coefficients. The least and highest computing times are achieved for the CRP1 with 10% wind penetration and CRP2 with 30% wind penetration, respectively. However, this range of average computing time remains acceptable for the hour-ahead planning framework.

VI. CONCLUSION

This paper has proposed a new PSCOPF formulation that accounts for failures of generating units and supports the optimization of their droop coefficients. It was shown that generator contingencies could lead to line overloads and thus

potentially to cascading outages, if they are not considered. Therefore, they must be included in the PSCOPF. Concerning the optimization of droop settings, since the exact model is a MILP with a large number of binary variables, it becomes computationally intractable even for the one-area IEEE RTS. Therefore, this paper proposes an approximate technique to find a solution more efficiently. The effectiveness and the benefit of droop coefficients optimization is demonstrated on the three-area IEEE RTS with different penetrations of wind generation. These simulations show that optimizing the droop coefficients significantly reduces the security cost. Furthermore, using the proposed PSCOPF model, we compare two CRP and conclude that wind integration reduces the overall effectiveness of the traditional CRP when balancing areas share the contingency reserve requirement. On the other hand, we show that the proposed PSCOPF model can be paired with the CRP proposed in [32] to achieve sizable reductions in the operating cost (up to 20.8% per operating interval) under high wind penetration levels.

Our future work will focus on improving the modelling aspects of this paper and its applicability in market-based power systems. Specifically, we will explore the possibility of modeling droop coefficients as continuous decision variables, thus avoiding the need to incorporate binary decision variables and use Benders decomposition. Similarly, we will investigate the impacts of out-of-market corrections, such as uplift and lost opportunity payments, which the optimized droop coefficients would incur in market-based power systems.

REFERENCES

[1] O. Alsac and B. Stott, "Optimal load flow with steady-state security," *IEEE Trans. Power App. Syst.*, vol. PAS-93, no. 3, pp. 745–751, May 1974.

[2] Q. Wang, J. D. McCalley, T. Zheng, and E. Litvinov, "A computational strategy to solve preventive risk-based security-constrained OPF," *IEEE Trans. Power Syst.*, vol. 28, no. 2, pp. 1666–1675, May 2013.

[3] Q. Wang and J. D. McCalley, "Risk and 'N-1' criteria coordination for real-time operations," *IEEE Trans. Power Syst.*, vol. 28, no. 3, pp. 3505–3506, Aug. 2013.

[4] B. Stott *et al.*, "Some key requirements for practical OPF calculation," in *Proc. FERC Conf.–Opportunities Increas. Real-Time Day-Ahead Market Effic. Through Improved Software*, 2012 [Online]. Available: http://goo.gl/bmC9vI

[5] PJM, "PJM manual 03: Transmission operations," 2015 [Online]. Available: http://www.pjm.com/~/media/documents/manuals/m03.ashx

[6] Y. Makarov *et al.*, "Blackout prevention in the United States, Europe, and Russia," *Proc. IEEE*, vol. 93, no. 1, pp. 1942–1955, Nov. 2005.

[7] F. Capitanescu *et al.*, "State-of-the-art, challenges, and future trends in security constrained optimal power flow," *Elect. Power Syst. Res.*, vol. 81, pp. 1731–1741, 2011.

[8] F. Capitanescu *et al.*, "Contingency filtering techniques for preventive security-constrained optimal power flow," *IEEE Trans. Power Syst.*, vol. 22, no. 4, pp. 1690–1697, Nov. 2007.

[9] Y. Li and J. McCalley, "Decomposed SCOPF for improving efficiency," *IEEE Trans. Power Syst.*, vol. 24, no. 1, pp. 494–495, Feb. 2009.

[10] A. Ardakani and F. Bouffard, "Identification of umbrella constraints in dc-based security-constrained optimal power flow," *IEEE Trans. Power Syst.*, vol. 28, no. 4, pp. 3924–3934, Nov. 2013.

[11] K. Karoui, H. Crisciu, and L. Platbrood, "Modeling the primary reserve allocation in preventive and curative security constrained OPF," in *Proc. IEEE PES Trans. Distrib. Conf. Expo.*, April 2010, pp. 1–6.

[12] Y. Wen and C. Guo, "Discussion on "solving preventive-corrective SCOPF by a hybrid computational strategy," *IEEE Trans. Power Syst.*, vol. 29, no. 6, pp. 3124–3124, Nov. 2014.

[13] Y. Xu *et al.*, "Solving preventive-corrective SCOPF by a hybrid computational strategy," *IEEE Trans. Power Syst.*, vol. 29, no. 3, pp. 1345–1355, May 2014.

[14] Y. Xu *et al.*, "Closure to discussion on "solving preventive-corrective SCOPF by a hybrid computational strategy," *IEEE Trans. Power Syst.*, vol. 29, no. 6, pp. 3124–3125, Nov. 2014.

[15] A. Wood and B. Wollenberg, *Power Generation, Operation, and Control*. Hoboken, NJ, USA: Wiley, 1984.

[16] Y. Rebours *et al.*, "A survey of frequency and voltage control ancillary services-Part I: Technical features," *IEEE Trans. Power Syst.*, vol. 22, no. 1, pp. 350–357, Feb. 2007.

[17] Y. Rebours *et al.*, "A survey of frequency and voltage control ancillary services MDASH; Part II: Economic features," *IEEE Trans. Power Syst.*, vol. 22, no. 1, pp. 358–366, Feb. 2007.

[18] Y. Dvorkin, D. Kirschen, and M. Ortega-Vazquez, "Assessing flexibility requirements in power systems," *IET Gen. Transm. Distrib.*, vol. 8, no. 11, pp. 1820–1830, 2014.

[19] ERCOT. (2010). *ERCOT Methodologies for Determining Ancillary Service Requirements* [Online]. Available: http://goo.gl/t2PHO2

[20] NERC. (2014). *Ancillary Services Matrix* [Online]. Available: http://goo.gl/IY3U42

[21] J. Restrepo and F. Galiana, "Unit commitment with primary frequency regulation constraints," *IEEE Trans. Power Syst.*, vol. 20, no. 4, pp. 1836–1842, Nov. 2005.

[22] R. Doherty, G. Lalor, and M. O'Malley, "Frequency control in competitive electricity market dispatch," *IEEE Trans. Power Syst.*, vol. 20, no. 3, pp. 1588–1596, Aug. 2005.

[23] E. Martinez Cesena, T. Capuder, and P. Mancarella, "Flexible distributed multienergy generation system expansion planning under uncertainty," *IEEE Trans. Smart Grid*, vol. 7, no. 1, pp. 348–357, Jan. 2016.

[24] SEC. "The Saudi Arabian grid code," 2007 [Online]. Available: https://www.se.com.sa/ar-sa/Lists/List/Attachments/1/SaudiArabianGridCode.pdf

[25] ENTSO-E, "Network code for requirements for grid connection applicable to all generators—Requirements in the context of present practices," 2012 [Online]. Available: https://www.entsoe.eu/major-projects/network-code-development/requirements-for-generators/Pages/default.aspx

[26] K. Folken *et al.*, "*Generator set adaptive droop control method*," U.S. Patent 20140265354 A1, 2014.

[27] B. Westphal and D. Stuebner, "*Steam turbine controller having method and apparatus for providing variable frequency regulation*," U.S. Patent 6250877 B1, 2001.

[28] C. Dozier *et al.*, "Generator set control system," U.S. Patent 20100102637 A1, 2013.

[29] G. Strbac and D. S. Kirschen, "Who should pay for reserve?" *Elect. J.*, vol. 13, no. 8, pp. 32–37, 2000.

[30] E. Ela *et al.*, "Market designs for the primary frequency response ancillary service-Part I: Motivation and design," *IEEE Trans. Power Syst.*, vol. 29, no. 1, pp. 421–431, Jan. 2014.

[31] E. Ela *et al.*, "Market designs for the primary frequency response ancillary service—Part II: Case studies," *IEEE Trans. Power Syst.*, vol. 29, no. 1, pp. 432–440, Jan. 2014.

[32] National Renewable Energy Laboratory, "Alternative approaches for incentivizing the frequency responsive reserve ancillary service," Tech. Rep. NREL/TP-5500-54393, 2012 [Online]. Available: http://www.nrel.gov/docs/fy12osti/54393.pdf

[33] E. Allen, J. Ingleson, and R. Schulz, "Monitored unit and system governing response to large frequency changes following loss of generation in normal operation system," in *Proc. IEEE Power Eng. Soc. Gener. Meeting*, Jun. 2007, pp. 1–14.

[34] J. Ingleson and E. Allen, "Tracking the eastern interconnection frequency governing characteristic," in *Proc. IEEE Power Eng. Soc. Gener. Meeting*, Jul. 2010, pp. 1–6.

[35] P. Du and Y. Makarov, "Using disturbance data to monitor primary frequency response for power system interconnections," *IEEE Trans. Power Syst.*, vol. 29, no. 3, pp. 1431–1432, May 2014.

[36] H. Illian, "Relating primary governing frequency response to future operating reliability," in *Proc. IEEE Power Eng. Soc. Gener. Meeting*, Jun. 2007, pp. 1–5.

[37] N. Jaleeli *et al.*, "Understanding automatic generation control," *IEEE Trans. Power Syst.*, vol. 7, no. 3, pp. 1106–1122, Aug. 1992.

[38] P. Kundur, *Power System Stability and Control*. New York, NY, USA: McGraw-Hill, 1994.

[39] Union for the Co-ordination of Transmission of Electricity (UCTE), *Operation Handbook*. 2004 [Online]. Available: https://www.entsoe.eu/publications/system-operations-reports/operation-handbook/Pages/default.aspx

[40] E. Lannoye, D. Flynn, and M. O'Malley, "Transmission, variable generation, and power system flexibility," *IEEE Trans. Power Syst.*, vol. 30, no. 1, pp. 57–66, Jan. 2015.

[41] Y. Dvorkin, H. Pandžić, M. Ortega-Vazquez, and D. Kirschen, "A hybrid stochastic/interval approach to transmission-constrained unit commitment with uncertainty," *IEEE Trans. Power Syst.*, vol. 30, no. 2, pp. 621–631, Mar. 2015.
[42] H. Pandžić, Y. Dvorkin, T. Qiu, Y. Wang, and D. Kirschen, "Toward cost-efficient and reliable unit commitment under uncertainty," *IEEE Trans. Power Syst.*, vol. 31, no. 2, pp. 970–982, Mar. 2016.
[43] J. Mohammadi, G. Hug, and S. Kar, "A Benders decomposition approach to corrective security constrained OPF with power flow control devices," in *Proc. IEEE Power Eng. Soc. Gen. Meeting*, Jul. 2013, pp. 1–5.
[44] J. Benders, "Partitioning procedures for solving mixed-variables programming problems," *Numer. Math.*, vol. 4, pp. 238–252, 1962/63.
[45] A. Geoffrion, "Generalized benders decomposition," *J. Optim. Theory Appl.*, vol. 10, no. 4, pp. 237–260, 1972.
[46] D. Bertsimas, E. Litvinov, X. A. Sun, Z. Jinye, and Z. Tongxin, "Adaptive robust optimization for the security constrained unit commitment problem," *IEEE Trans. Power Syst.*, vol. 28, no. 1, pp. 52–63, Feb. 2013.
[47] H. Pandžić *et al.*, "Unit commitment under uncertainty—GAMS models," *Lib. Renew. Energy Anal. Lab (REAL)*, Univ. Washington, Seattle, WA, USA Tech. Rep., 2014 [Online]. Available: http://www.ee.washington.edu/research/real/gams_code.html
[48] (2014). *IBM ILOG CPLEX Optimizer* [Online]. Available: http://goo.gl/pPFo5j
[49] R. Rosenthal, *GAMS-A User's Guide*. Washington, DC, USA: GAMS Development Corporation, 2013 [Online]. Available: http://www.gams.com/help/topic/gams.doc/userguides/GAMSUsersGuide.pdf
[50] H. Pandžić, T. Qiu, and D. Kirschen, "Comparison of state-of-the-art transmission constrained unit commitment formulations," in *Proc. IEEE Power Eng. Soc. Gener. Meeting*, Jul. 2013, pp. 1–5.
[51] D. Lew *et al.*, "*The western wind and solar integration study–NREL/TP-5500*," Nat. Renew. Energy Lab., Denver, CO, USA, Tech. Rep., 2010 [Online]. Available: http://www.nrel.gov/electricity/transmission/western_wind.html
[52] H. Pandžić, Y. Wang, T. Qiu, Y. Dvorkin, and D. Kirschen, "Near-optimal method for siting and sizing of distributed storage in a transmission network," *IEEE Trans. Power Syst.*, vol. 30, no. 5, pp. 2288–2300, Sep. 2015.

Yury Dvorkin (S'11) received the B.S.E.E degree (with the highest Hons.) from Moscow Power Engineering Institute (Technical University), Moscow, Russia, in 2011. He is currently working toward the Ph.D. degree in electrical engineering at the University of Washington, Seattle, WA, USA.

Previously, he was a Graduate Intern with the Center for Nonlinear Studies, Los Alamos National Laboratory, Los Alamos, NM, USA. His research interests include short- and long-term planning in power systems with renewable generation and power system economics.

Mr. Dvorkin was the recipient of the Clean Energy Institute Graduate Fellowship (2013–2014) and the Clean Energy Institute Student Training and Exploration Grant (2014–2015).

Pierre Henneaux (S'11–M'14) received the M.Sc. degree in engineering physics and the Ph.D. degree in applied sciences from the Universite Libre de Bruxelles (ULB), Brussels, Belgium, in 2009 and 2013, respectively.

Since October 2014, he has been a Power System Engineer with the Tractebel Engineering (ENGIE), Brussels, Belgium. Prior to joining Tractebel Engineering, he was an F.R.S-FNRS Research Fellow at the ULB and a Research Associate with the University of Washington with a fellowship of the Belgian American Educational Foundation. His research interests include reliability of power systems and blackout risk analysis.

Daniel S. Kirschen (M'86–SM'91–F'07) received the Ingénieur Civil Mécanicien Electricien degree in electrical and mechanical engineering from the Universite Libre de Bruxelles, Brussels, Belgium, and the M.Sc. and Ph.D. degrees in electrical engineering from the University of Wisconsin, Madison, WI, USA, in 1979, 1980, and 1985, respectively.

He is currently a Close Professor of Electrical Engineering with the University of Washington, Seattle, WA, USA. His research interests include smart grids, the integration of renewable energy sources in the grid, power system economics, and power system security.

Hrvoje Pandžić (S'06–M'12) received the M.E.E. and Ph.D. degrees in electrical engineering from the Faculty of Electrical Engineering and Computing, University of Zagreb, Zagreb, Croatia, in 2007 and 2011, respectively.

From 2012 to 2014, he was a Postdoctoral Researcher with the University of Washington, Seattle, WA, USA. Currently, he is an Assistant Professor with the Faculty of Electrical Engineering and Computing, University of Zagreb. His research interests include planning, operation, control, and economics of power and energy systems.